Supporting information

Pre-embedding Energetic Metal-Organic Framework to Create Interconnected Pore Structures in Nitrogen-doped Carbon for Green and Effective Hydrogen Peroxide Electrosynthesis

Yuyu Guo,[a‡] Jinxi Han,[a‡] Shuting Li,[a] Zhengqiang Xia,[a] Sanping Chen,[a*] Gang Xie,[a] Shengli Gao,[a] Qi Yang[a*]

[a] *Key Laboratory of Synthetic and Natural Functional Molecule of the Ministry of Education, College of Chemistry and Materials Science, Northwest University, Xi'an, Shaanxi, 710127, China.*

**Corresponding authors e-mail address: yangqi@nwu.edu.cn, sanpingchen@126.com*

[‡] *These authors have equal contribution to this work.*

Experimental section

Materials

5-Amino-1*H*-tetrazole (CH_3N_5, 98%), Zinc nitrate hexahydrate ($Zn(NO_3)_2·6H_2O$, 99%), acetonitrile (CH_3CN, 99%), cyanuric chloride ($C_3Cl_3N_3$, 99%), ethanol (C_2H_5O, 99.5%), sucrose ($C_{12}H_{22}O_{11}$, 99.5%), polyacrylamide (M_r=2000000-14000000) and 2-methylimidazole ($C_4H_6N_2$, 98%) were acquired form Shanghai Aladdin Biochemical Technology Co., Ltd. Nitric acid (HNO_3, 65%), hydrochloric acid (HCl, 37%) and acetone (C_3H_6O, 99.5%) were acquired from Sinopharm.

Synthetic process

Synthesis of H_3TATT and EMOF $\{[Zn_2(HTATT)_2(H_2O)_2]·3H_2O\}_n$

The synthesis of H_3TATT *and* EMOF $\{[Zn_2(HTATT)_2(H_2O)_2]·3H_2O\}_n$ was according to our previous work[1].

Synthesis of carbon aerogel (CA)

40 ml of H_2O were combined with 5.5 g of sucrose, 1 g polyacrylamide, and agitated for 24 hours. The mixture was transferred to a 50 ml Teflon reactor and sealed with a stainless steel case. It was heated to 200 °C, kept for five hours, and then allowed to naturally cool to room temperature. The obtained gel was freeze-dried for 24 hours and ground to achieve black powder. A porcelain boat containing 1g of the obtained powder was heated to 950 °C for two hours under N_2 atmosphere, with a heating rate of 5 °C per minute, and cooling down to room temperature naturally.

Synthesis of CA-Zn

The synthesis process is the same as that of section 2.2.2, except that added 1.49 g $Zn(NO_3)_2·6H_2O$.

Synthesis of CA-ZIF8

The synthesis process is the same as that of section 2.2.2, except that added 1.49 g $Zn(NO_3)_2·6H_2O$ and 1.64 g 2-methylimidazole.

Synthesis of CA-NR

The synthesis process is the same as that of section 2.2.2, except that added 1.4 g H_3TATT and 0.71 g $Zn(NO_3)_2·6H_2O$.

Electrochemical measurements

The electrochemical measurements were carried out on corrtest bipotentiostat (CS2350) using three-electrode system. A rotary ring disk electrode with glass carbon (GC, 4mm) was used as working electrode. A saturated calomel electrode was used as

reference electrode. A graphite rod was used as the counter electrode. The electrolyte uses 0.1 M KOH solution. The catalyst (5 mg) dispersed in the mixed solution of deionized water (900 μL), ethanol (90 μL) and 5% Nafion (10 μL), then ultrasonic for 30 min under an ice bath to form a homogeneous catalyst ink. Next, 10 μL ink was dropped on the GC carefully and dried at room temperature. Before electrochemical measurements, the electrolyte was bubbled with gases for 30 min to obtain electrolyte saturated with N_2 and O_2. Cyclic voltammetry (CV) was performed in electrolyte at a scan rate of 20 mV s^{-1}. Linear sweep voltammetry (LSV) was performed at different rotating rates (400, 625, 900, 1225, 1600, 2025 and 2500 rpm) with a scan rate of 20 mV s^{-1}. Electrochemical double layer capacitance (C_{dl}) was tested in the non-Faraday region with different scan rates. All the obtained potentials were transformed to reversible hydrogen electrode (RHE) by the following equation: $E_{RHE}=E_{Ag/Cl}+0.059pH+0.197$ V. Electron transfer number (n) and H_2O_2 yield (%) were obtained based on the following equation:

$$H_2O_2(\%) = \frac{200 \times I_r}{N \times I_d + I_r}$$

$$n = \frac{4 \times I_d}{I_d + \frac{I_r}{N}}$$

where I_r and I_d are the ring and disk currents, respectively, and N (0.47) is the current collection efficiency.

The faradaic efficiency on RRDE was obtained as the following equation:

$$FE\% = 100 \times \frac{\frac{I_r}{N}}{I_d}$$

Bulk H_2O_2 production test was conducted by chronoamperometry with different potential in H-Cell. The electrocatalyst was supported on carbon paper (1×1 cm^2, Toray), the electrocatalyst loading was 1 mg cm^2.

The concentration of produced H_2O_2 was calculated by the $Ce(SO_4)_2$ titration method as following reaction:

$$2Ce^{4+} + H_2O_2 \rightarrow 2Ce^{3+} + 2H^+ + O_2$$

The Ce^{4+} was reduction by produced H_2O_2 and generated the colorless Ce^{3+}. The produced concentration of H_2O_2 can be calculated as following:

$$C(H_2O_2) = \frac{V_{Ce^{4+}} \times C_{Before}Ce^{4+} - (V_{Ce^{4+}} + V_{removedelectrolyte}) \times C_{after}Ce^{4+}}{2 \times V_{removedelectrolyte}}$$

The production rate of H_2O_2 can be calculated as following:

$$H_2O_2\ Productionrate = \frac{C_{H_2O_2} \times V_{electrolyte}}{A \times t}$$

The FE of bulk synthesis of H_2O_2 can be calculated as following:

$$FE(\%) = \frac{C_{H_2O_2} \times V_{electrolyte} \times 2 \times 96485}{\int_0^t idt}$$

Physical characterization

The phase composition and structure of all samples were obtained on X-ray diffraction (XRD, Bruker D8 advance, Cu Kα radiation, λ = 0.15418 nm). The morphology details were observed by scanning electron microscopy (SEM, Apreo S, Thermo Fisher Scientific) and transmission electron microscopy (TEM, JEM 2100F) with energy dispersive X-ray spectrometer. Thermal decomposition information was acquired from thermal gravimetry analysis (TG, STA 449C, Netzsch Co.) using N_2 gas as the atmosphere. The specific surface area was tested and calculated using Brunauer-Emmett-Teller (BET, TriStar II 3020, Micromeritics) method. Samples were vacuum degassed at 150 ℃ for 6 hours. The Raman spectra recorded on a Micro-Raman imaging spectrometer (Raman, DXR2, Thermo Fisher Scientific). The chemical composition and valence were detected by X-ray photoelectron spectroscopy (XPS, PHI 5000 VersaProbe III, ULVAC-PHI).

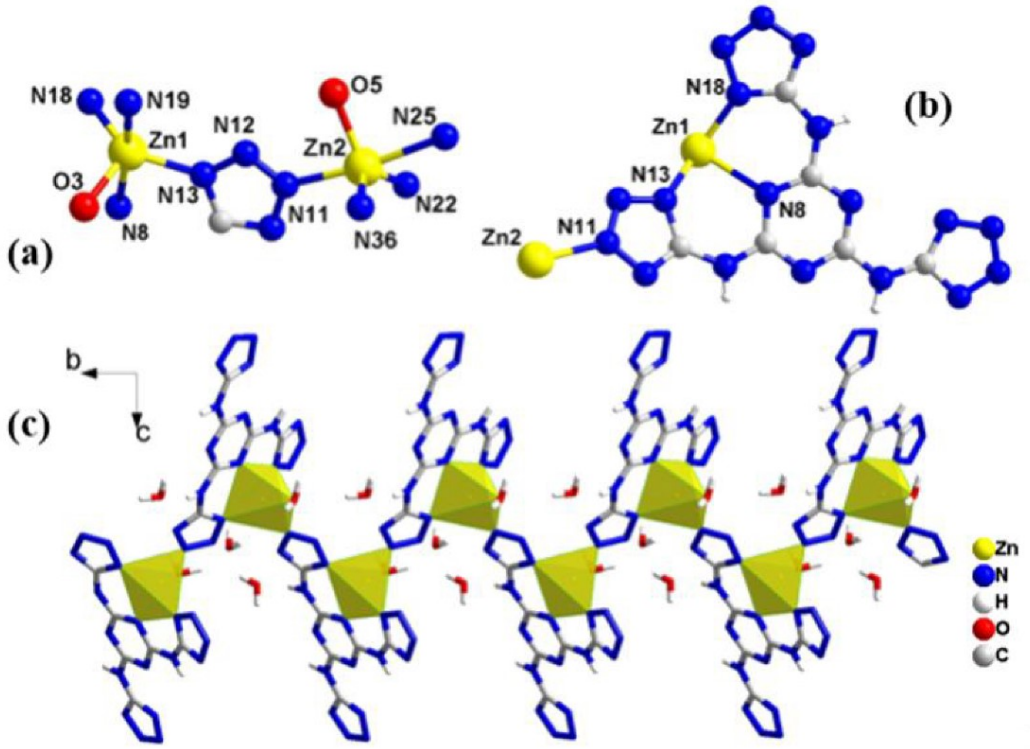

Figure S1. Crystal structure of $\{[Zn_2(HTATT)_2(H_2O)_2]\cdot 3H_2O\}_n$

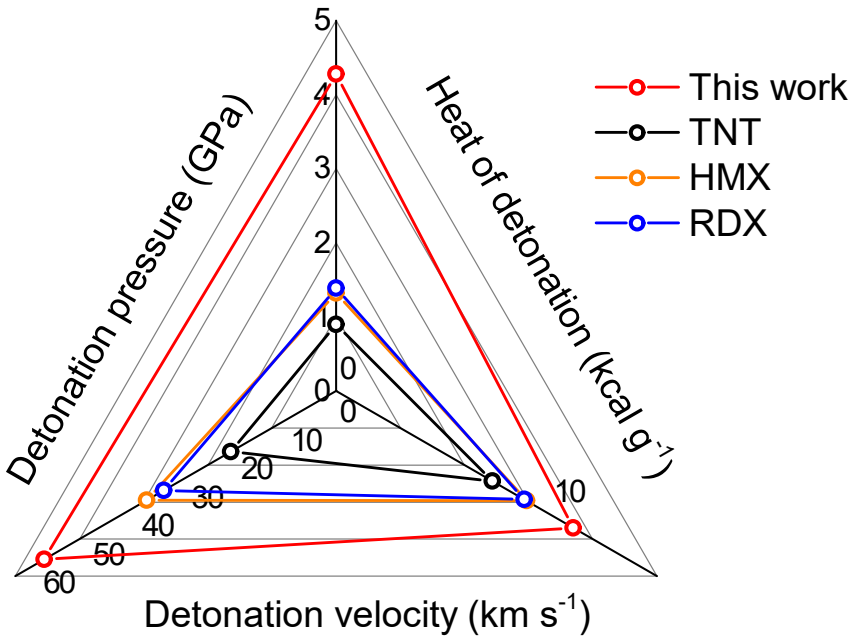

Figure S2. Comparison of detonation data with some classical energetic materials.

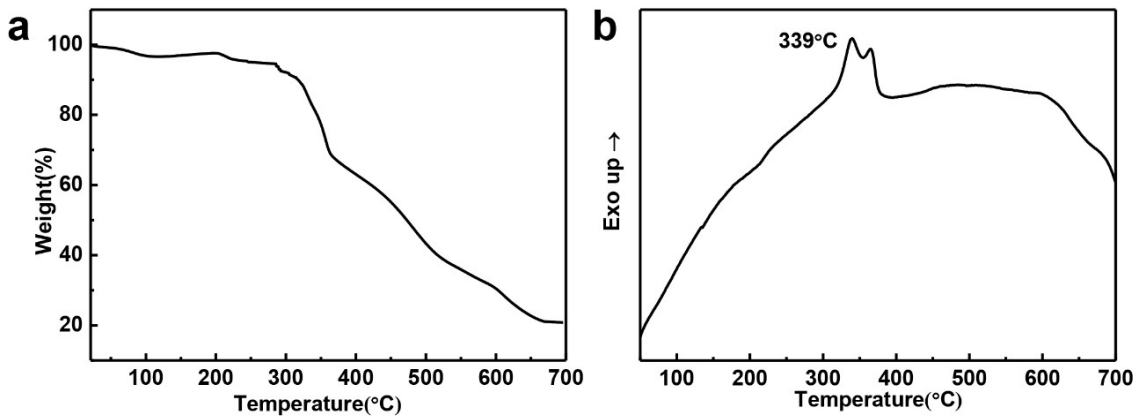

Figure S3. a) TG and b) spectrum of $\{[Zn_2(HTATT)_2(H_2O)_2]\cdot 3H_2O\}_n$

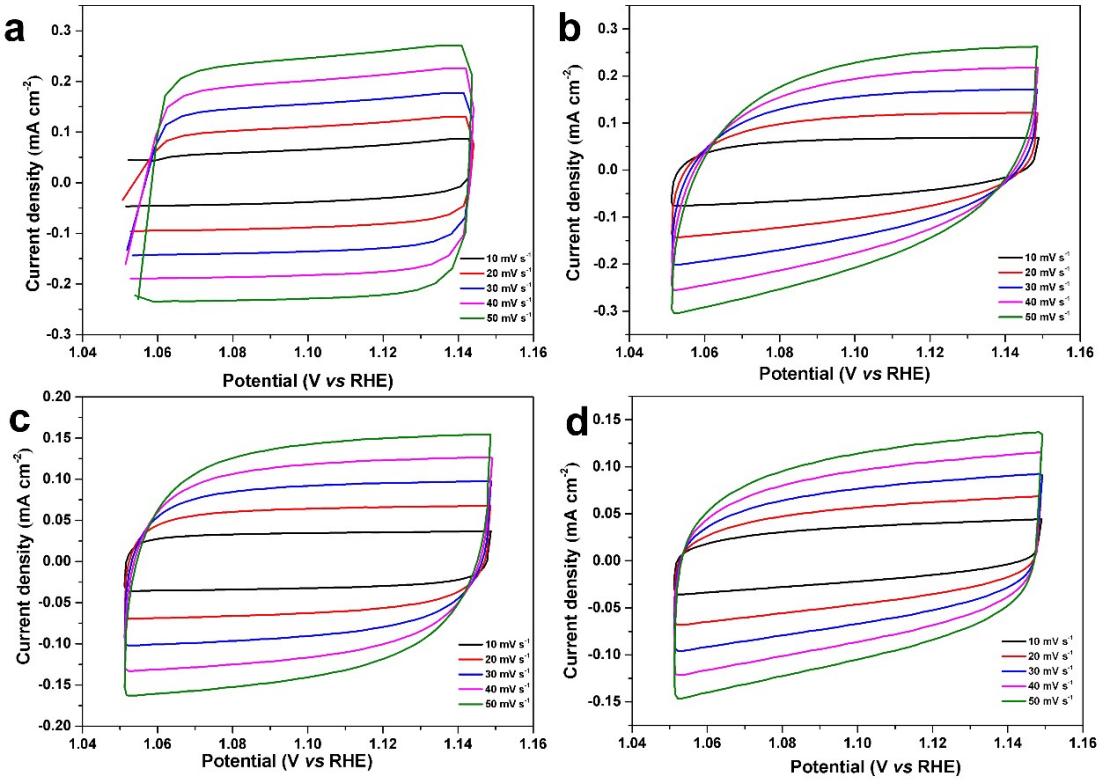

Figure S4. CV curves of a) CA-NR. b) CA-ZIF8. c) CA-Zn and d) CA in the non-faraday region at different rates.

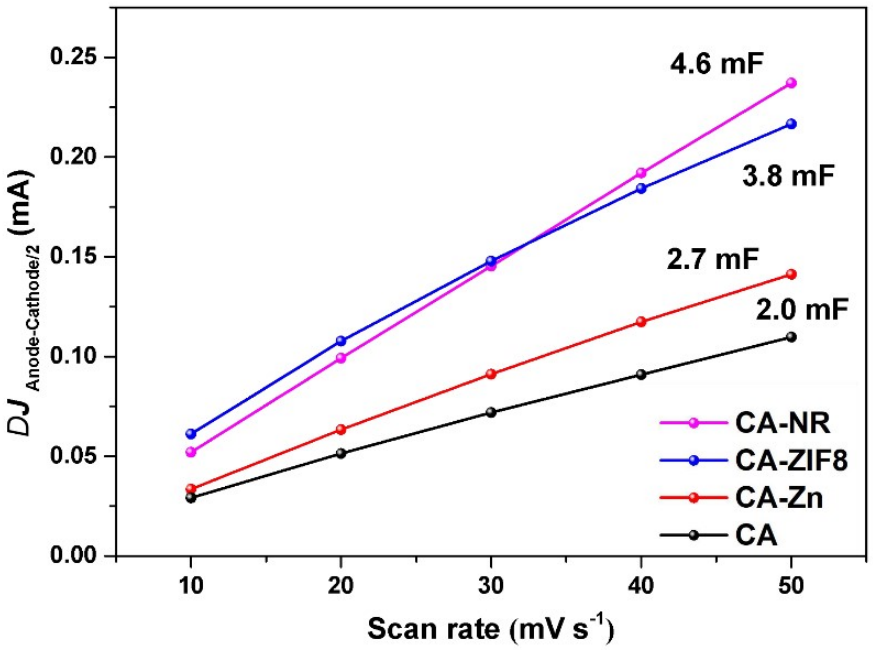

Figure S5. Linear fitting of the capacitive current for samples.

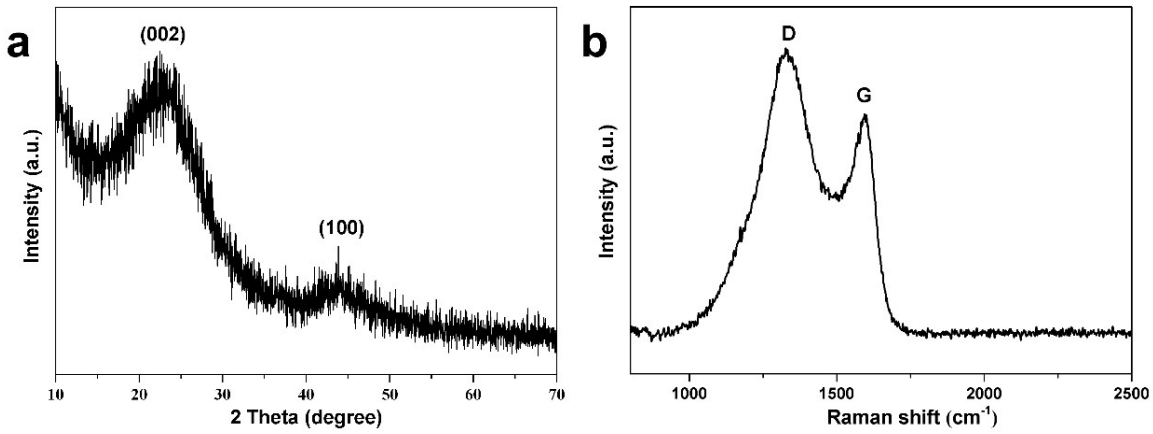

Figure S6. XRD and Raman spectrum of CA-NR after long time test.

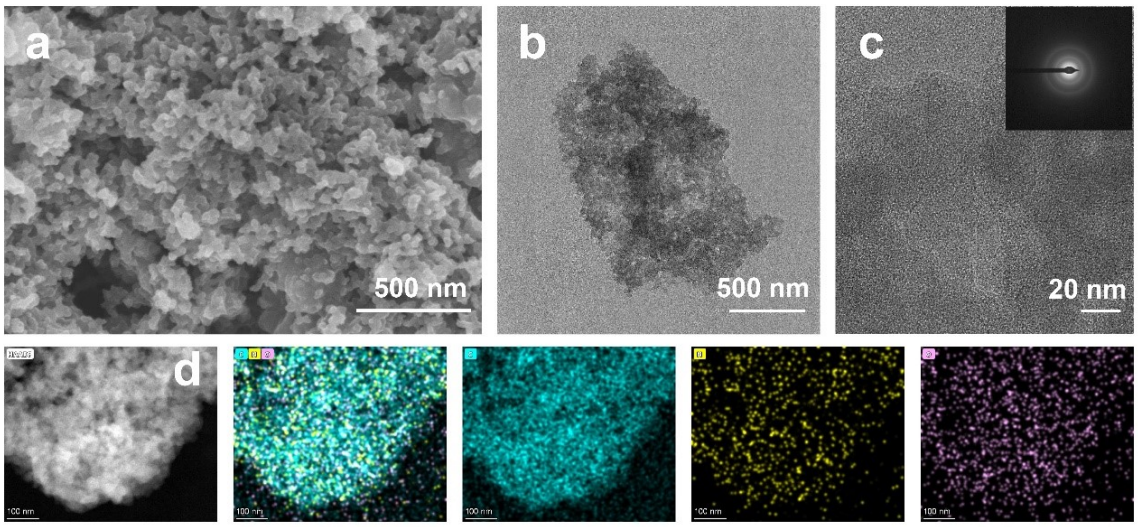

Figure S7. a) SEM. b) TEM. c) HRTEM and d) HAADF-STEM images of CA-NR.

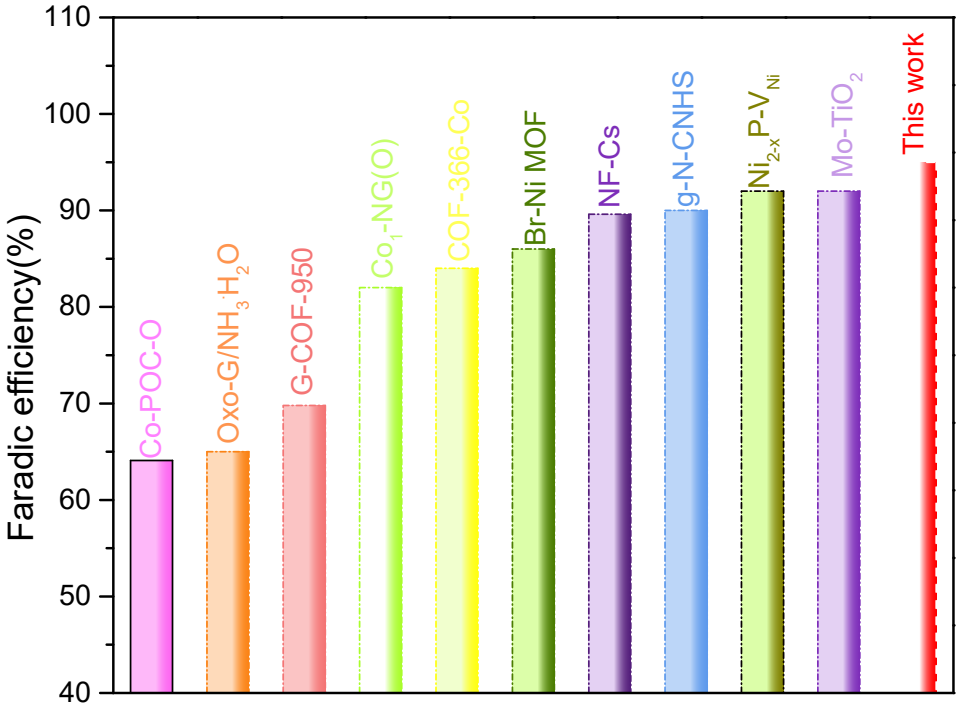

Figure S8. Comparison of faradic efficiency with recently reported catalysts[2-11].

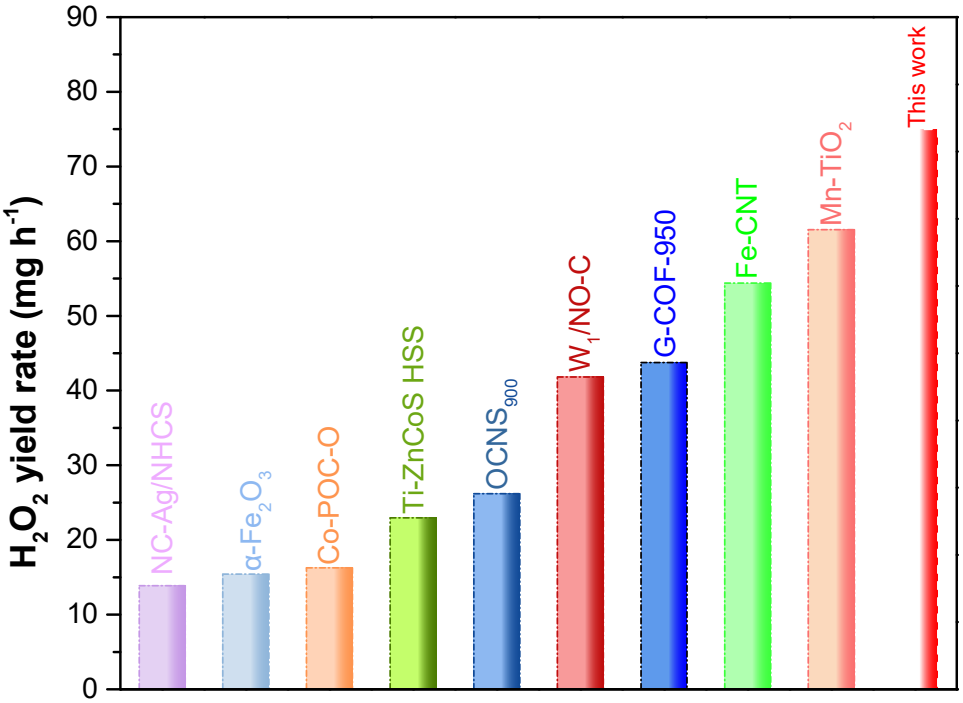

Figure S9. Comparison of H_2O_2 yield with recently reported catalysts[4, 6, 12-18].

Table S1. Physicochemical data of $\{[Zn_2(HTATT)_2(H_2O)_2]\cdot 3H_2O\}_n$ and some classical energetic materials.

	ρ[a] (g cm^{-3})	N[b] (%)	T_d[c] (^oC)	Q[d] (kcal g^{-1})	D[e] (km s^{-1})	P[f] (GPa)	IS[g] (J)	FS[h] (N)
$\{[Zn_2(HTATT)_2(H_2O)_2]\cdot 3H_2O\}_n$	1.980	57.58	364	4.279	11.09	59.10	>40	>360
$[Pb(HBTI)]_n$[19]	3.186	34.22	325	1.158	7.84	35.87	>40	>360
$[Cu(Htztr)_2(H_2O)_2]_n$[20]	1.892	52.72	345	2.128	8.18	30.57	>40	>360
$[Cu(tztr)]\cdot H_2O$[20]	2.316	45.23	325	1.322	7.92	31.99	>40	>360
$[Cu(Htztr)]_n$[20]	2.435	49.08	355	3.958	10.40	56.48	32	>360
CHP[21]	1.95	14.71	194	1.25	8.225	31.73	0.5	-
CHHP[22]	2.00	28.25	231	0.75	6.205	17.96	0.8	-
TNT[23]	1.65	18.50	295	0.897	7.303	21.30	15.0	353
RDX[23]	1.80	37.84	205	1.386	8.795	34.90	7.5	120
HMX[23]	1.91	37.84	275	1.320	8.900	38.39	7.0	112

[a] Density from X-ray diffraction analysis, [b] Nitrogen content, [c] Temperature of decomposition by DSC, [d] Heat of detonation, [e] Detonation velocity, [f] Detonation pressure, [g] Impact sensitivity, [h] Friction sensitivity, CHP = Cobalt hydrazine perchlorate, CHHP = Cobalt hydrazine hydrazinecarboxylate perchlorate.

Reference

1. S. Wu, M. Li, Z. Yang, Z. Xia, B. Liu, Q. Yang, Q. Wei, G. Xie, S. P. Chen, S. L. Gao, J. Y. Lu *Green Chem.,* 2020, **22**, 5050-5058.
2. L. Han, Y. Sun, S. Li, C. Cheng, C. E. Halbig, P. Feicht, J. L. Huebner, P. Strasser, S. Eigler, *ACS Catal.,* 2019, **9**, 1283-1288.
3. N. Jia, T. Yang, S. Shi, X. Chen, Z. An, Y. Chen, S. Yin, P. Chen, *ACS Sustainable Chem. Eng.,* 2020, **8**, 2883-2891.
4. B. Q. Li, C. X. Zhao, J. N. Liu, Q. Zhang, *Adv. Mater.,* 2019, **31**, 1808392.
5. Z. Zhou, Y. Kong, H. Tan, Q. Huang, C. Wang, Z. Pei, H. Wang, Y. Liu, Y. Wang, S. Li, X. Liao, W. Yan, S. Zhao, *Adv. Mater.* 2022, **34**, 2106321.
6. J. Zhang, G. Zhang, S. Jin, Y. Zhou, Q. Ji, H. Lan, H. Liu, J. Qu, *Carbon*, 2020, **163**, 154-161.
7. Z. Deng, C. Ma, S. Yan, J. Liang, K. Dong, T. Li, Y. Wang, L. Yue, Y. Luo, Q. Liu, Y. Liu, S. Gao, J. Du, X. Sun, *Catal. Sci. Technol.,* 2021, **11**, 6970-6974.
8. D. Iglesias, A. Giuliani, M. Melchionna, S. Marchesan, A. Criado, L. Nasi, M. Bevilacqua, C. Tavagnacco, F. Vizza, M. Prato, P. Fornasiero, *Chem*., 2018, **4**, 106-123.
9. M. Liu, Y. Li, Z. Qi, H. Su, W. Cheng, W. Zhou, H. Zhang, X. Sun, X. Zhang, Y. Xu, Y. Jiang, Q. Liu, S. Wei, *J. Phys. Chem. Lett.,* 2021, **12**, 8706-8712.
10. C. Liu, H. Li, F. Liu, J. Chen, Z. Yu, Z. Yuan, C. Wang, H. Zheng, G. Henkelman, L. Wei, Y. Chen *J. Am. Chem. Soc.,* 2020, **142**, 21861-21871.
11. E. Jung, H. Shin, B. H. Lee, V. Efremov, S. Lee, H. S. Lee, J. Kim, W. Hooch Antink, S. Park, K. S. Lee, S. P. Cho, J. S. Yoo, Y. E. Sung, T. Hyeon, *Nat. Mater.,* 2020, **19**, 436-442.
12. K. Jiang, S. Back, A. J. Akey, C. Xia, Y. Hu, W. Liang, D. Schaak, E. Stavitski, J. K. Norskov, S. Siahrostami, H. Wang, *Nat. Commun.,* 2019, **10**, 3997-4002.
13. M. Jin, W. Liu, J. Sun, X. Wang, S. Zhang, J. Luo, X. Liu, *Nano Res.,* 2022, **15**, 5842-5847.
14. S. Chen, T. Luo, K. Chen, Y. Lin, J. Fu, K. Liu, C. Cai, Q. Wang, H. Li, X. Li, J. Hu, H. Li, M. Zhu, M. Liu, *Angew. Chem. Int. Edit.,* 2021, **60**, 16607-16614.
15. Y. Wang, Y. Xue, C. Zhang, *Electrochim. Acta,* 2021, **368**, 138385.
16. Q. Chen, C. Ma, S. Yan, J. Liang, K. Dong, Y. Luo, Q. Liu, T. Li, Y. Wang, L. Yue, B. Zheng, Y. Liu, S. Gao, Z. Jiang, W. Li, X. Sun, *ACS Appl. Mater. Inter.,* 2021, **13**, 46659-46664.
17. F. Zhang, Y. Zhu, C. Tang, Y. Chen, B. Qian, Z. Hu, Y. C. Chang, C. W. Pao, Q. Lin, S. A. Kazemi, Y. Wang, L. Zhang, X. Zhang, H. Wang, *Adv. Funct. Mater.,* 2022, **32**, 2112433.
18. R. Gao, L. Pan, Z. Li, C. Shi, Y. Yao, X. Zhang, J. J. Zou, *Adv. Funct. Mater.,* 2020, **30**, 1907716.
19. Q. Yang, G. L. Yang, W. Zhang, S. Zhang, Z. Y. Yang, G. Xie, Q. Wei, S. P. Chen, S. L. Gao, *Chem. Eur. J.,* 2017, **23**, 9149-9155.
20. X. Y. Liu, W. J. Gao, P. P. Sun, Z. Y. Su, S. P. Chen, Q. Wei, G. Xie, S. L. Gao, *Green Chem.,* 2015, **17**, 831-836.
21. O. S. Bushuyev, P. Brown, A. Maiti, R. H. Gee, G. R. Peterson, B. L. Weeks, L. J. Hope-Weeks, *J. Am. Chem. Soc.,* 2012, **134**, 1422-1425.
22. O. S. Bushuyev, G. R. Peterson, P. Brown, A. Maiti, R. H. Gee, B. L. Weeks, L. J. Hope-Weeks, *Chem. Eur. J.,* 2013, **19**, 1706-1711.
23. J. K. Rudolf Meyer, A. Homburg, F. Matter, Index. In *Explosives*, 2007.